Physica 127B (1984) 282–291
North-Holland, Amsterdam

KINETIC THEORY OF THE EIGENMODES OF CLASSICAL FLUIDS AND NEUTRON SCATTERING

E.G.D. COHEN
The Rockefeller University, 1230 York Avenue, New York, NY 10021, USA

I.M. DE SCHEPPER
Interuniversitair Reactor Instituut, 2629 JB Delft, The Netherlands

M.J. ZUILHOF
Instituut voor Theoretische Fysica, Rijksuniversiteit Utrecht, 3508 TA Utrecht, The Netherlands

The lowest lying eigenmodes of a classical fluid have been approximately determined for a wide range of densities and wavenumbers. The most important eigenmodes are direct extensions of the three hydrodynamic heat and sound modes to much larger wavenumbers. A new and consistent interpretation of neutron spectra and related molecular dynamics simulations in terms of these modes is made. Also experimental predictions are discussed, some of which seem particularly suitable for investigating with spallation sources.

1. Introduction

We have studied the most important–lowest lying–eigenmodes of a hard sphere fluid as a function of density on the basis of kinetic theory. These eigenmodes allow us to obtain information about all correlation functions of the fluid, in particular $S(k, \omega)$. The study of the behavior of these eigenmodes as a function of k, the comparison of the theoretical $S(k, \omega)$ and related functions with computer results for various inter-particle potentials, as well as with experimental data for liquid Ar, He, Rb, H_2, etc., has lead to a new interpretation of many aspects of the neutron spectra of fluids. In particular, it allows one, in principle, to follow in detail the change in $S(k, \omega)$ from a function dominated by collective eigenmodes for small k and ω to one dominated by individual particle modes for large k and ω. It has also led to a number of predictions about $S(k, \omega)$ of real fluids, some of which have already been confirmed experimentally, and it has raised a number of questions that could be answered in part by experiments with the new neutron spallation sources.

Of all the correlation functions of the fluid, we will restrict ourselves here to the density–density correlation function or its Fourier transform, the intermediate scattering function $F(k, t)$ or its double Fourier transform, the dynamic structure factor $S(k, \omega)$.

2. Kinetic theory

Our starting point is an approximate linear kinetic operator that determines the time evolution of all the correlation functions in the fluid, in particular the $S(k, \omega)$ [1]. This operator is a generalization to high densities of the linearized Boltzmann operator in the spirit of one made many years ago by Enskog. It is only applicable to a fluid of hard spheres, since the collisions are supposed to be instantaneous. For hard spheres of diameter σ this (inhomogeneous generalized) Enskog operator $L(k)$ is a sum of three terms: a free-streaming term, a collision term and a mean field term:

$$L(k) = -ik \cdot v + ng(\sigma)\Lambda_k + nA_k. \tag{1}$$

Here k is a wave vector, v the velocity, $g(\sigma)$ the

radial distribution function of two spheres at contact, n the number density, Λ_k is a binary collision operator defined on a function $h(v)$ by

$$\Lambda_k h(v) = -\sigma^2 \int d\hat{\sigma} \int dv' \psi(v') g \cdot \hat{\sigma} \theta(g \cdot \hat{\sigma}) \times [h(v) - h(v^*) + e^{-ik\cdot\sigma}\{h(v') - h(v'^*)\}], \quad (2)$$

while the mean field operator A_k, which contains the static correlations in the fluid through the static structure factor $S(k)$, is defined by

$$A_k h(v) = [C(k) - g(\sigma) C_0(k)] \times \int dv' \psi(v') ik \cdot v' h(v'). \quad (3)$$

In (2) and (3) $\hat{\sigma}$ is a unit vector ($\sigma = \sigma\hat{\sigma}$), $g = v - v'$, $\theta(x)$ the unit step function, $v^* = v - g \cdot \hat{\sigma}\hat{\sigma}$ and $v'^* = v' + g \cdot \hat{\sigma}\hat{\sigma}$ are the velocities of the restituting collision, the direct correlation function $C(k) = n^{-1}[1 - 1/S(k)]$, $C_0(k)$ is its low density limit and $\psi(v) = (\beta m/2\pi)^{3/2} \times \exp(-\beta m v^2/2)$, where m is the mass of a hard sphere and $\beta = 1/k_B T$ with T the temperature and k_B Boltzmann's constant.

The application of $L(k)$ is through a spectral decomposition in eigenmodes:

$$L(k) = -\sum_j |\Psi_j(k, v)) z_j(k) (\Phi_j(k, v)|, \quad (4)$$

where each $z_j(k)$ denotes an eigenvalue of $-L(k)$ and Ψ_j and Φ_j are the corresponding right and left eigenfunctions respectively. The bracket notation in (4) refers to the inner product $\langle f | g \rangle = \langle f^* g \rangle = \int dv f(v) f^*(v) g(v)$. With the eqs. (1)–(4) one has:

$$S(k, \omega) = \frac{1}{\pi} S(k) \mathrm{Re} \left\langle \frac{1}{i\omega - L(k)} \right\rangle = \frac{1}{\pi} S(k) \mathrm{Re} \sum_j \frac{A_j(k)}{i\omega + z_j(k)}, \quad (5)$$

where $A_j(k) = \langle \Psi_j(k, v) \rangle \langle \Phi_j^*(k, v) \rangle$. The first equality in (5) suggests that $S(k, \omega)$ can be determined directly from $L(k)$, the second equality gives a representation of $S(k, \omega)$ as an infinite sum of Lorentzians.

To determine the $z_j(k)$ explicitly, Λ_k in (1), (2) is approximated by operators $\Lambda_k^{(M)}$ labeled by an integer M and defined by

$$\Lambda_k^{(M)} = \sum_{j,l=1}^{M-1} |\phi_j) \Omega_{jl}(k) (\phi_l| + \Omega_{MM}(k) [1 - P_{M-1}], \quad (6)$$

where $\{\phi_l\}$ is a complete set of suitably chosen orthonormal polynomials in v, P_M projects on $\phi_1 \cdots \phi_M$ and $\Omega_{jl}(k) = \langle \phi_j^* \Lambda_k \phi_l \rangle$. By choosing $M = 7, \ldots, 11$ convergent results have been obtained for the first six eigenmodes.

The time evolution of the self-correlation functions in the fluid are governed by the Lorentz–Enskog operator $L^s(k)$ defined by

$$L^s(k) = -ik \cdot v + n g(\sigma) \Lambda_\infty, \quad (7)$$

where $\Lambda_\infty = \lim_{k\to\infty} \Lambda_k$, i.e., Λ_∞ is given by (2) without the last two terms on the right-hand side. The spectral decomposition of $L^s(k)$ can be made in a completely similar manner as for $L(k)$ and since $L(k)$ tends to $L^s(k)$ for large k ($\lim_{k\to\infty} A_k = 0$), the eigenmodes of $L(k)$ will tend to those of $L^s(k)$. For all k the eigenmodes of $L(k)$ can be divided into two classes: the five extended hydrodynamic modes and the kinetic modes; the first are those that go to zero for $k \to 0$ and are generalizations to large k of the well-known hydrodynamic modes of hydrodynamics. The kinetic modes all approach non-zero positive values for $k \to 0$. We are interested here mainly in the heat mode $j = h$ and the two sound modes $j = \pm$. For $L^s(k)$ there is only one hydrodynamic mode: a self-diffusion mode $j = D$. Important is that the eigenvalue $z_h(k)$ of $L(k)$ tends to the self-diffusion eigenvalue $z_D(k)$ of $L^s(k)$, which for small k, in the hydrodynamical regime, are given by $z_h(k) = \alpha_E k^2$ and $z_D(k) = D_E k^2$, where α_E and D_E are the thermal diffusivity and the self-diffusion coefficient given by the Enskog transport theory. The half width $\omega_H(k)$ of $S(k, \omega)$, defined in general by

$$S(k, \omega_H(k)) = \tfrac{1}{2} S(k, 0), \quad (8)$$

can be computed directly for the hard sphere fluid using (5) and (8). Similar considerations hold for $S_s(k, \omega)$, given by

$$S_s(k, \omega) = \frac{1}{\pi} \mathrm{Re} \left\langle \frac{1}{i\omega - L^+(k)} \right\rangle. \tag{9}$$

3. Eigenvalues for a hard sphere fluid

The lowest six eigenmodes have been studied [2] for a range of densities varying from $V_0/V = 0.05$ to 0.650, where $V_0 = N\sigma^3/\sqrt{2}$ is the volume of close packing. The three extended hydrodynamic modes describe $S(k, \omega)$ well up to $kl_E \approx 0.6$ where the mean free path $l_E = \sigma/2\pi \times (V_0/V)g(\sigma)$, i.e., for $V_0/V = 0.3$ up to $k\sigma = 2$ and for $V_0/V = 0.625$ up to $k\sigma = 12$. With three more (kinetic) modes, a good description of $S(k, \omega)$ is obtained up to $kl_E \approx 1.5$, i.e., for $V_0/V = 0.3$ up to $k\sigma \approx 5$ for $V_0/V = 0.625$ up to $k\sigma \approx 30$.* In the region where the three extended hydrodynamic modes suffice, a Landau–Placzek-like description of $S(k, \omega)$ is possible, as a sum of three Lorentzians [1], or equivalently, a generalized hydrodynamic description obtains with k-dependent thermodynamic and transport coefficients, as discussed by Alder c.s. [3, 4]. The eigenvalues $z_j(k)$ behave, as a function of k, quite differently from what one would expect from a simple generalization of their hydrodynamic equivalents, which are $\sim k^2$ for their real (damping) parts and $\sim k$ for their imaginary (propagating) parts. Our study of the eigenmodes reveals the following.

a) *Heat mode.* The extended heat mode eigenvalue $z_h(k)$, is always real, and ≥ 0, i.e., the heat mode is always purely damped. Moreover, it is the most important of all the eigenmodes. It determines *the height* $S(k, 0)$ and the *halfwidth* $\omega_H(k)$ of $S(k, \omega)$ [1], as well as the long-time behavior of $F(k, t)$ since it is the lowest lying mode. $z_h(k)$ is sketched in fig. 1 for $V_0/V = 0.25$, and 0.50 and together with ω_H for $V_0/V = 0.625$ in fig. 2. Like all other modes, $z_h(k)$ exhibits an oscillatory behavior as a function of k around an

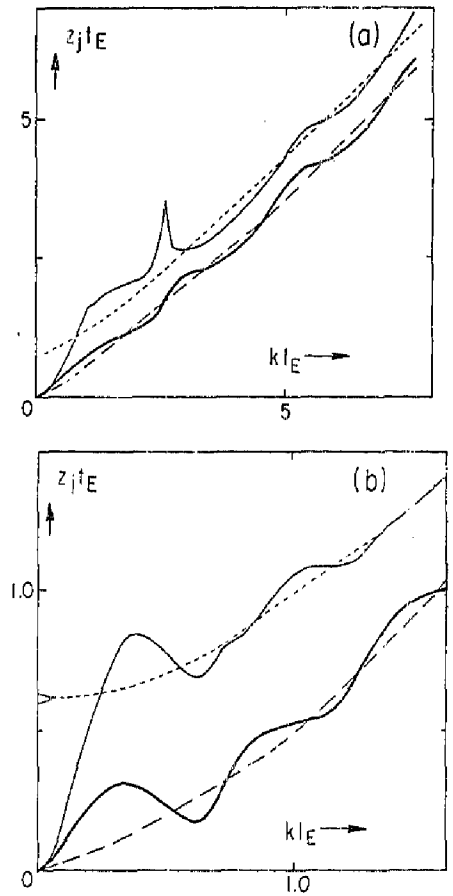

Fig. 1. Reduced heat mode $z_h t_E$ (——) and sound damping $z_s t_E$ (——) as a function of the reduced wave number kl_E for the densities $V_0/V = 0.25$ (a) and 0.50 (b). The heat mode and the sound damping oscillate around the self-diffusion mode $z_D t_E$ (———) and a kinetic mode (– – –) of $L^+(k)$, respectively. Here $t_E(l_E)$ are the Enskog mean free time (path).

* On comparing a real fluid with a hard sphere fluid, a choice of an effective diameter for the hard sphere fluid has to be made. At a given temperature the effective diameter was determined as the average of those values of σ for which respectively the location and the height of the first maximum of $S(k)$ of both fluids coincide. Then $\sigma \approx 3$–4 Å and for most experiments $V_0/V \approx 0.52$–0.65.

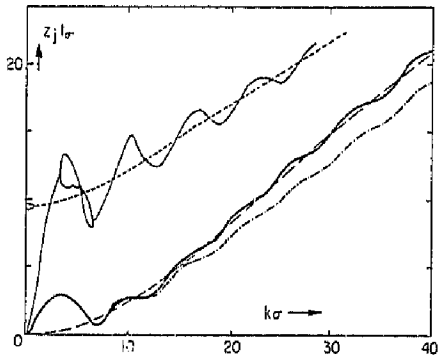

Fig. 2. Reduced heat mode $z_h t_\sigma$ (——), sound damping $z_s t_\sigma$ (——) and half width $\omega_H t_\sigma$ (– · –) as a function of $k\sigma$ for $V_0/V = 0.625$. The sound damping is double-valued where the sound dispersion exhibits a gap (cf. fig. 5e). Also shown are the self-diffusion mode $z_D(k)t_\sigma$ (——) and a kinetic mode (– – –) of L^*. Here $t_\sigma = (\beta m)^{1/2}\sigma/2$.

eigenmode (in this case $z_D(k)$) of $L^*(k)$. The oscillations in $z_h(k)$ are generated by $S(k)$ as well as by the factor $e^{-ik\cdot\sigma}$ in Λ_k.

For $V_0/V > 0.30$ a minimum in $z_h(k)$ as a function of k occurs that becomes more and more pronounced with increasing density. For the same densities a minimum in $\omega_H(k)$ occurs, the de Gennes minimum. We shall discuss the behavior of $z_h(k)$ and its connection with $\omega_H(k)$ in detail for $V_0/V = 0.625$ but the arguments are valid for *all* $V_0/V > 0.30$.

The minimum of $z_h(k)$ and $\omega_H(k)$ both occur at $k = k_G$ such that $k_G\sigma \approx 2\pi$ (or $\lambda \approx \sigma$). An approximate expression for $z_h(k)$ for $0 < kl_E < 0.6$ or $0 < k\sigma < 12$, can be obtained by perturbation theory [2] and reads

$$z_h(k) = \frac{D_E k^2}{S(k)}\, d(k) + \mathcal{O}((kl_E)^4). \tag{10}$$

Here $d(k) = \langle \phi_2 \Lambda_k^{-1} \phi_2 \rangle / \langle \phi_2 \Lambda_\infty^{-1} \phi_2 \rangle$ (with $\phi_2 = (\beta m)^{1/2} \hat{k} \cdot v$) is independent of the density and characterizes the oscillations of Λ_k around Λ_∞. Eq. (10) implies that while $z_h(k)$ oscillates around $z_D(k) \approx D_E k^2$, $S(k)$ causes a sharp minimum in $z_h(k)$ at $k = k_G \approx k_S$, where k_S is that k where $S(k)$ has a maximum. However, the oscillations due to $S(k)$ alone are too large and are considerably corrected by the dynamic factor

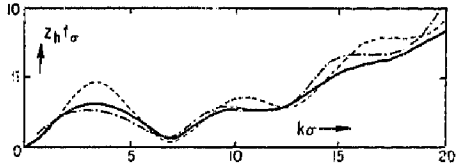

Fig. 3. Reduced heat mode $z_h t_\sigma$ (——) and the approximations $D_E k^2 t_\sigma / S(k)$ (– – –) and $D_E k^2 t_\sigma d(k)/S(k)$ (– · – · –) as a function of the reduced wavenumber $k\sigma$ for $V_0/V = 0.625$.

$d(k)$. We note that with increasing k, $k^2/S(k)$ gets increasingly out of phase with $z_h(k)$, which is corrected by $d(k)$ (cf. fig. 3).

While for $k\sigma \lesssim 12$, $S(k)$ dominates and codetermines the minimum of $z_h(k)$, for $k\sigma \gtrsim 30$, Λ_k dominates. For intermediate values of $k\sigma$ ($12 \lesssim k\sigma \lesssim 30$) a (destructive) interference between the oscillations of $S(k)$ and Λ_k occurs. As a consequence, for $k \gtrsim k_G$, the oscillations of $z_h(k)$ around $z_D(k)$–and to a lesser extent those of $\omega_H(k)$ around $\omega_H^S(k)$–decrease and then increase again (cf. fig. 2). The approach of the heat mode to the self-diffusion mode, for $k \gtrsim k_G$ (cf. fig. 2), can physically be understood as a consequence of the disappearance at these and larger values of k (i.e., for $\lambda \lesssim \sigma$) of four of the five local conservation laws and the (approximate) validity of only one conservation law still, namely that of the conservation of mass.

Since–like in hydrodynamics–$S(k, 0)$ is inversely proportional to $\omega_H(k)$, the qualitative features discussed here for $\omega_H(k)$ also hold for $S(k, 0)$. In particular, $S(k, 0)$ exhibits a very sharp maximum at $k = k_G$.

We remark that with decreasing density the difference $|k_G - k_s|$ grows (cf. fig. 4), the De Gennes minimum flattens out and disappears for $V_0/V \approx 0.30$. We also note that $z_h(k_G)$ is remarkably linear as a function of the density (cf. fig. 4) even up to $V_0/V = 0.7$, where the hard sphere fluid is undercooled.*

* We note that the $z_h(k_G)$ for liquid argon at 120 K for five densities, as well as that of other substances, all lie on the same straight line, when appropriately reduced. This line extrapolates to a reduced density of $V_0/V = 0.745$, close to the reduced melting densities of Ar and hard spheres of $V_0/V = 0.735$. This raises the question whether the vanishing of $z_h(k_G)$ is connected with the disappearance of an undercooled fluid state.

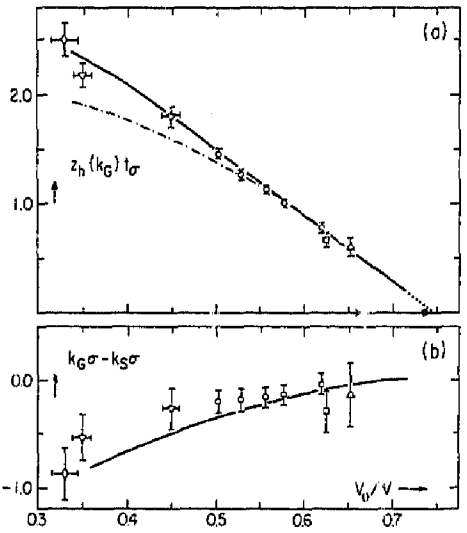

Fig. 4. Density dependence of (a) $z_h(k_G)$ (–) and $\omega_H(k_G)$ (– · –), where $z_h(k)$ and $\omega_H(k)$ have their (de Gennes) minimum at $k = k_G$; and (b) difference between $k_G\sigma$ and $k_S\sigma$, where $S(k)$ has its first maximum at $k = k_S$. Experimental values for $z_h(k_G)$ of Ar (○) at 120 K, $\sigma = 3.43$ Å, $t_\sigma = 1.03$ ps [5, 9]; and for $\omega_H(k_G)$ of Ar (□) at 85 K, $\sigma = 3.46$ Å, $t_\sigma = 1.30$ ps [18]; Rb (△) at 315 K; $\sigma = 4.44$ Å, $t_\sigma = 1.27$ ps [10]; Kr (▽) at 297 K; $\sigma = 3.59$ Å, $t_\sigma = 1.05$ ps [19] and He (◇) at 4.2 K, $\sigma = 2.92$ Å, $t_\sigma = 1.56$ ps [8] are also inserted. The bars indicate estimated uncertainties. In (a), the reduced solidification (×) and melting (·) densities for a hard sphere fluid and for Ar at 120 K, which coincide, are also indicated.

The long-time behavior of the intermediate scattering function $F(k, t)$ is given entirely by the heat mode, i.e., then $F(k, t) \sim e^{-z_h(k)t}$. Corrections due to other modes become increasingly important with decreasing values of t and increasing values of k (see below sub c).

b) *Sound modes.* The extended sound mode eigenvalues are each other's complex conjugate: $z_\pm = \pm i\omega_s + z_s$. They are in general propagating modes, i.e., $\omega_s \neq 0$, that are damped, i.e., $z_s \geq 0$. However, they are not always visible in $S(k, \omega)$ as *separate maxima*, as they are in the hydrodynamic regime, where they appear as separate lines. This does *not* mean that they are absent, but only that their contribution is not directly observable. For a hard sphere fluid they are visible as separate maxima for $k\sigma \leq 0.5$. The most interesting behavior again occurs at high (liquid) densities. Starting at $V_0/V \geq 0.52$, the two sound modes show a *propagation gap* for certain values of k, where $\omega_s = 0$ and the modes do not propagate (fig. 5). In such a region there are two purely damped (non-propagating) modes that oscillate around a kinetic mode of L^s (cf. fig. 2). The location of this region is around $k\sigma \approx 2\pi$, i.e., $\lambda \approx \sigma$, and the existence of the gap and the behavior of ω_s around the gap are both very little dependent on $S(k)$.*

Physically, the appearance of a gap is caused by a competition between elastic (restoring) and dissipative forces, which for sufficiently small k (for instance, in the hydrodynamic regime, where the former are $\sim k\sigma$ and the latter $\sim (k\sigma)^2$) are always won by the elastic forces, so that propagation of sound occurs. For larger k, however, the dissipative forces prevail for certain ranges of k-values, so that no propagation is possible. The disappearance of the gap for still larger k-values is due to the free streaming term $-ik \cdot v$, which represents free propagation. This limits the number of propagation gaps to one ($0.52 \leq V_0/V \leq 0.55$ and $0.625 \leq V_0/V \leq 0.680$) or two ($0.55 \leq V_0/V \leq 0.625$ and $0.68 \leq V_0/V \leq 0.70$) at most. With decreasing density, the gap disappears below $V_0/V \approx 0.52$, when, first, a Landau-like dispersion curve appears for $0.50 \geq V_0/V \geq 0.40$, till finally for $V_0/V \leq 0.20$ a monotonically rising line with very slowly changing slope appears (cf. fig. 5). Like the heat mode minima, so does the propagation gap manifest itself in the form of $S(k, \omega)$ as a function of k, albeit in a more subtle way. For k-values corresponding to the gap, the contributions to $S(k, \omega)$ will shift from the shoulders to the center, there being three real (damped) modes now. Thus, for liquid densities, where both phenomena occur around $k\sigma \approx 2\pi$, not only a narrow but also a relatively sleek line will appear for such k-values.

c) *Kinetic modes.* All the eigenvalues of the kinetic modes in this theory are positive for

* In general, the behavior of the sound modes—both the real (damping) part and the imaginary (propagating) part depend weakly on $S(k)$, this contrary to the behavior of the heat mode.

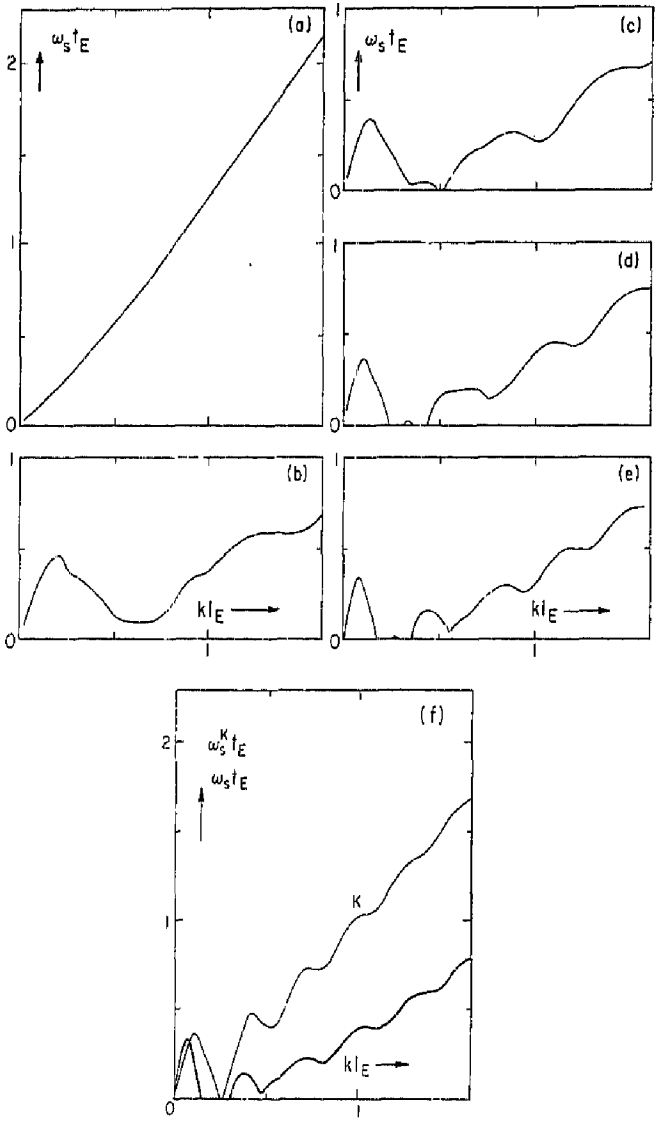

Fig. 5. Reduced sound dispersion $\omega_s t_E$ as a function of kl_E for $V_0/V = 0.10$ (a); 0.45 (b); 0.525 (c); 0.575 (d); 0.625 (e) and 0.650 (f). One or more propagation gaps appear for $V_0/V \geq 0.52$. In (f) a kinetic mode ω_s^K of $L(k)$ with a propagation gap is also plotted.

$k \to 0$, i.e., damped and non-propagating. Of the lowest three, one is always real the other two are almost degenerate at $k = 0$ and become complex, i.e., propagating already for $kl_E > 0.005$. At very high densities ($V_0/V \geq 0.650$) the dispersion curve of these propagating kinetic modes also exhibits a propagation gap, just as occurred for the sound modes [2] (fig. 5f).

The kinetic modes are important for a proper description of $F(k, t)$ at short times or $S(k, \omega)$ for large ω, especially at large k. For instance, for $V_0/V = 0.625$, our $F(k, t)$, determined from the Enskog theory and that of Alder c.s. determined from MD are both well described with the three extended hydrodynamic modes alone for all t as long as $k\sigma \leq 1.0$. For $1 \leq k\sigma < 9$, these same three modes describe $F(k, t)$ well for $t/t_E \geq 2$, while for $9 \leq k\sigma \leq 30$, this only obtains for $t/t_E \geq 3.5$ [2]. With six modes a good description is obtained for all t up until $k\sigma = 30$.

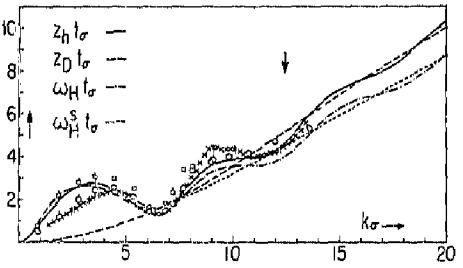

Fig. 6. Reduced heat mode $z_h t_\sigma$ for liquid Ar at 120 K and 115 bar (×); for a comparable Lennard-Jones (LJ) fluid (○); for a repulsive Lennard-Jones (RLJ) fluid at the same temperature (□) and for hard spheres according to the generalized Enskog theory (——) as a function of $k\sigma$. Also, the reduced halfwidths $\omega_H t_\sigma$ (– · –) and $\omega_H^s t_\sigma$ (– – – –) and the reduced self-diffusion mode $z_D t_\sigma$ (— —) are plotted as a function of $k\sigma$. The arrow points to that value of $k\sigma$ where $kl_E = 1$. In all cases, $V_0/V = 0.53$.

4. Real fluids

4.1. Present experiments

The results for hard sphere fluids suggest a new way of interpreting neutron spectra of real fluids, viz. in terms of the eigenmodes of the fluids. In general, although there are quantitative differences in certain cases, the qualitative picture seems to remain valid. Molecular dynamics (MD) calculations of $S(k, \omega)$ and a decomposition of $S(k, \omega)$ in three Lorentzians (cf. eq. (5)) support the idea that the quantitative differences that do occur between hard sphere and real fluids, are mainly due to the difference in interparticle potential but not due to physically different processes. Thus, by making for the $S(k, \omega)$ of liquid Argon such a decomposition in three Lorentz lines [5]–which suffices for the accuracy with which *any* $S(k, \omega)$ has been obtained so far, either experimentally or by MD [6]–the extended heat mode and sound modes can be determined for $k\sigma \leq 14$ (cf. figs. 6, 7). Then one finds that the extended heat mode of liquid Ar determines $S(k, 0)$ [1] and in particular the halfwidth ω_H completely [1, 7], resembles very much that derived from a MD-calculation for a 12–6

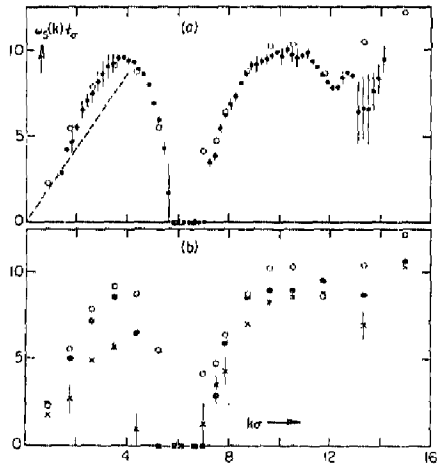

Fig. 7. a) Reduced sound frequency $\omega_s t_\sigma$ as a function of $k\sigma$ for liquid Ar at 120 K and 115 bar (·) and a comparable LJ system (○) with $k_B T/\varepsilon = 0.97$. The dashed curve represents $\omega_s = ck$ with $c = 715\ \mathrm{ms}^{-1}$. b) The same for a LJ (○) and a RLJ (●) system at $k_B T/\varepsilon = 0.97$ and a RLJ (×) system at $k_B T/\varepsilon = 3.90$. Note the propagation gap around $k\sigma \approx 2\pi$ where $\omega_s = 0$.

Lennard-Jones fluid [6] and is also close to that of an 'equivalent' hard sphere gas [1, 7]. An exception is the region $k\sigma \lesssim 4$, where the hard sphere results differ considerably both in magnitude and in shape. A MD-calculation with a steep purely repulsive (RLJ)–but not hard sphere–potential (see ref. 6) shows agreement with the $\omega_H(k)$ of the hard sphere fluid. These differences in ω_H can be understood on the basis of eq. (10) and the difference in $S(k)$ for the two fluids, which is due to their different interparticle potentials (cf. fig. 6). A similar comparison of $\omega_H(k)$ of liquid helium at 4.20 K with the heat mode of an equivalent hard sphere gas ($V_0/V = 0.33$; $\sigma = 2.92$ Å) also shows good agreement between the two [2, 8].

Like for hard spheres, one finds for liquid argon at 120 K and 20, 115, 270 and 400 bar, a large, slightly density dependent sound propagation gap around $k\sigma \approx 2\pi$ [5, 9]. The magnitude and shape of the dispersion curves are very similar to those determined by MD for a 12–6 Lennard–Jones fluid (cf. fig. 7) but are quite different from that of an equivalent hard sphere fluid. However, again, a MD-calculation with a RLJ potential suggests that this difference is due to the difference in interparticle potential (cf. fig. 7) [6]. The k-values for which separate sound peaks become *visible* in various liquids depends on the interparticle potential. For liquid Ar it is for $k\sigma \lesssim 1$ [1], while for liquid Rb already for $k\sigma \lesssim 4$ [10] peaks are distinguishable.

4.2. Future experiments

Experiments performed at larger values of k and ω than hitherto available could check to what extent the hard sphere results also carry over to the regime $kl_E > 1$ or approximately $k\sigma \gtrsim 10$ for real fluids.

1) In general, with decreasing density the importance of individual particle effects, due to $i\boldsymbol{k}\cdot\boldsymbol{v}$, will increase at the expense of collective effects that are due to A_k and A_k. In fact, the smaller the density, the smaller the value of $k\sigma$ for which $kl_E > 1$. Consequently, the effects discussed in the following two points can be studied much better at low than at high densities and spallation sources could perhaps be used to particular advantage.

2) Thus, one could wonder whether also *six Lorentzians* (three extended hydrodynamical modes and three kinetic modes (one with real and two with complex conjugate eigenvalues)) would suffice to describe $S(k, \omega)$ consistently as a function of ω for $1 < kl_E < 2$. One would expect that as long as $\omega < t_s^{-1}$, where t_s is an average time to tranverse the steep part of the interparticle potential [11], the behavior would qualitatively resemble that of a hard sphere fluid, but that for $\omega > t_s^{-1}$ differences would occur. This seems to be borne out by experiments on liquid Ar [9] and liquid H_2 [12].

3) The transition to *ideal gas behavior*, i.e., where $S(k, \omega)$ becomes a Gaussian in ω with width $\sim k$, is unclear, even for hard spheres. Whether this change takes place via the incoherent scattering function $S_s(k, \omega)$ or that both functions approach ideal gas behavior simultaneously, and how – if at all – the (infinite) sum of Lorentzians on the right hand side of (5) approaches a Gaussian, are all open questions. Thus, the transition from collective to individual particle behavior is not clear at present. It should be remarked that the *first* correction to the Gaussian form of $S(k, \omega)$, has been computed exactly for a hard sphere fluid [11]. Approximate calculations of this correction have also been made for a 12–6 Lennard-Jones fluid [12, 13].

4) It would be interesting to investigate the *universality* of a propagation gap for fluids at sufficiently high densities and the occurrence of a Landau-like dispersion curve at lower fluid densities. Thus liquid Ar at appropriate *lower* densities than hitherto considered should exhibit a Landau-like dispersion curve, while at sufficiently *high* densities–outside the temperature and density region usually considered in low temperature physics–helium should exhibit a propagation gap [14]. One can also ask whether the propagation gap is *unique* for fluids. Since such a gap also appears in a continuum model of a fluid based on the Navier–Stokes equations [15], it appears that the fluidity or diffusivity of a fluid as opposed to the rigidity of a glass or a solid might be essential.

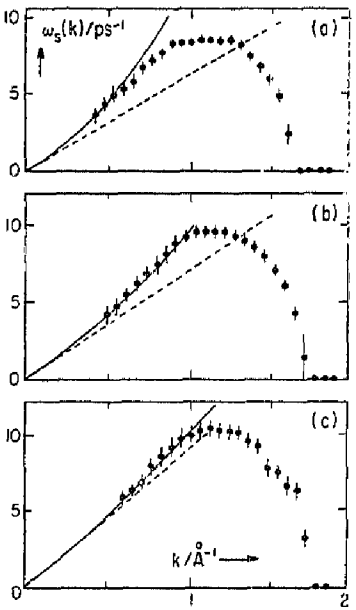

Fig. 8. Positive anomalous sound dispersion of ω_s (in ps^{-1}) as a function k (in Å^{-1}) for liquid Ar at 120 K and three pressures: (a): 20 bar, $c = 613$ ms^{-1}, $a = 1.04$ Å$^{3/2}$; (b): 115 bar, $c = 715$ ms^{-1}, $a = 0.36$ Å$^{3/2}$; (c): 400 bar, $c = 898$ ms^{-1}, $a = 0.105$ Å$^{3/2}$, compared with $\omega_s = ck$ (dashed line) and mode coupling theory $\omega_s = ck[1 + ak^{3/2}]$ (solid line).

5) For liquid Argon, the approach of the dispersion curve to the hydrodynamic regime, i.e., to ck, (c is the velocity of sound) is from above, i.e., there is positive anomalous dispersion for liquid Argon, (cf. fig. 8) [5, 9]. The behavior of this anomalous dispersion is very well described numerically by mode-coupling theory [16]:

$$\omega_s(k) = ck[1 + ak^{3/2}], \tag{11}$$

when the constant a is computed using the experimental values for thermodynamic and transport properties of Argon. Why the mode-coupling theory should be applicable to $k\sigma \approx 3$ is an open question. A similar positive dispersion has been observed for liquid helium at 1.2 K (fig. 9) [17]. In that case, a classical hard sphere calculation with $\sigma \approx 3$ Å yields $a = 0.18$ Å$^{3/2}$ and gives a perfect fit. The physical significance of this–if any–is unclear at present.

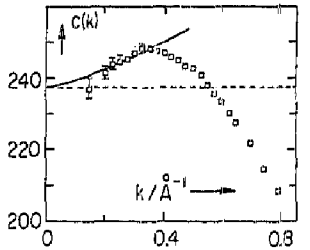

Fig. 9. Positive anomalous phase velocity $c(k) = \omega_s/k$ (in ms^{-1}) as a function of k (in Å^{-1}) for liquid helium at 1.2 K and saturated vapor pressure (□) compared with the velocity of sound $c = 238$ ms^{-1} (dashed line) and with mode coupling theory for a classical hard sphere fluid with $\sigma = 3$ Å and $a = 0.18$ Å$^{3/2}$ (solid line).

References

[1] I.M. de Schepper and E.G.D. Cohen, Phys. Rev. A22 (1980) 287; J. Stat. Phys. 27 (1982) 223.
[2] I.M. de Schepper, E.G.D. Cohen and M.J. Zuilhof, Phys. Lett. 101A (1984) 399; 103A (1984) 120.
[3] W.E. Alley and B.J. Alder, Phys. Rev. A27 (1983) 3158.
[4] W.E. Alley, B.J. Alder and S. Yip, Phys. Rev. A27 (1983) 3174.
[5] I.M. de Schepper, P. Verkerk, A.A. van Well and L.A. de Graaf, Phys. Rev. Lett. 50 (1983) 974.
[6] I.M. de Schepper, J.C. van Rijs, A.A. van Well, P. Verkerk, L.A. de Graaf and C. Bruin, Phys. Rev. A29 (1984) 1602.
[7] I.M. de Schepper, J.C. van Rijs, A.A. van Well, P. Verkerk, L.A. de Graaf and C. Bruin, Poster, 4th CMD Conf., E.P.S., The Hague (1984).
[8] A.D.B. Woods, E.C. Svensson and P. Martel, Can. J. Phys. 56 (1978) 302.
[9] I.M. de Schepper, P. Verkerk, A.A. van Well and L.A. de Graaf, Phys. Lett. 104A (1984) 29.
[10] J.R.D. Copley and J.M. Rowe, Phys. Rev. A9 (1974) 1656.
[11] I.M. de Schepper, M.H. Ernst and E.G.D. Cohen, J. Stat. Phys. 25 (1981) 321.
[12] V.F. Sears, Phys. Rev. A5 (1972) 452; Phys. Rev. A7 (1973) 340.
[13] H.H.U. Konijnendijk, Short time behavior of density correlation functions, Thesis, Delft (1977) p. 80.

[14] L.A. de Graaf, private communication.
[15] J.C. van Rijs, I.M. de Schepper and E.G.D. Cohen, to be published.
[16] M.H. Ernst and J.R. Dorfman, J. Stat. Phys. 12 (1975) 311.
[17] W.G. Stirling, Annual Report ILL (1981) p. 179.
[18] K. Sköld, J.M. Rowe, G. Ostrowski and P.D. Randolph, Phys. Rev. A6 (1972) 1107.
[19] P.A. Egelstaff, W. Glaser, D. Litchinsky, E. Schneider and J.-B. Suck, Phys. Rev. A27 (1983) 1106.